Int. J. Rock Mech. Min. Sci. Vol. 8, pp. 165–178. Pergamon Press 1971. Printed in Great Britain

AN EXACT SOLUTION TO THE RADIALLY END-CONSTRAINED CIRCULAR CYLINDER UNDER TRIAXIAL LOADING

B. T. BRADY

Denver Mining Research Center, Bureau of Mines, Denver, Colorado

(*Received* 8 *November* 1969)

Abstract—An exact theoretical solution is presented for the stresses and displacements in a radially end-constrained elastic cylindrical specimen deformed axially between cylindrical end-plates of different elastic properties from those of the specimen. The exact solution for the stresses and displacements is expressed by a Fourier series representation. The solution is exact in the sense that the stresses are expressed by series and become exact in the limit as more terms are used.

There are four boundary conditions that are satisfied by the solution: (1) The radial and tangential stresses are equal to zero and/or to the value of the radial pressure applied to the surface of the specimen; (2) the shear stress is zero at *all* points along the cylindrical surface of the specimen; (3) the ends of the specimen remain plane while being subjected to a resultant applied axial force; (4) the radial displacement along the ends of the specimen is specified by the functional relation $g(r)$, where r is a radial distance always less than or equal to the radius of the specimen. It is shown that the functional form of this relationship is determined by the elastic properties (Young's modulus and Poisson's ratio) and geometry of the specimen and end-plates.

The solution is used to solve the problem of the deformation of a specimen compressed axially between rough end-plates (no slippage between the contact surfaces) of the same diameter as the specimen.

INTRODUCTION

A PROCEDURE commonly used in experimental rock and soil mechanics research involves the use of a circular cylindrical specimen loaded axially between rough end-plates† [1, 2]. It is known that this test procedure is somewhat unsatisfactory because of the development of a nonuniform stress distribution throughout the specimen resulting from an elastic mismatch between the specimen and end-plates‡ [3–6]. Consequently, mechanical property values (Young's modulus, Poisson's ratio, rupture strength, etc.) are affected both by the geometry of the test specimen (length-to-diameter ratio, L/D) and by the magnitude of the radial constraint arising at the interface between the specimen and end-plates. A quantitative solution to this problem can provide useful information both in understanding the mechanics of the problem and in serving as a guide to designing a test specimen in

† In a test specimen loaded between rough end-plates, there is no relative movement between the specimen and end-plate at the contact surface.

‡ A convenient measure of the magnitude of the elastic mismatch is the ratio $(\nu_p/E_p)/(\nu_s/E_s)$, where ν and E are Poisson's ratio and Young's modulus and the subscripts s and p refer to the specimen and end-plate, respectively. For most tests in which steel end-plates are used $(\nu_s/E_s) > (\nu_p/E_p)$, which implies that the specimen tends to expand radially more than the end-plates. Because of the frictional restraint offered by the end-plates, shearing stresses develop at the contact between the specimen and end-plate. These stresses act inward for compression testing and produce a 'clamping' effect. The effect of this 'clamping' is to produce a state of triaxial stress throughout the specimen.

which a somewhat uniform state of stress exists throughout the specimen during the test. Such a design will enable accurate measurements of the intrinsic mechanical properties of the specimen.

A number of quantitative studies have been made of the effect of radial end-constraint on the elastic behavior of a cylindrical test specimen compressed axially between rough end-plates [1; 3–11]. These studies can be grouped into two distinct classes—experimental and theoretical. We are concerned chiefly in this paper with the theoretical aspect of the problem of radial end-constraint. The results of the experimental studies have beeu reported elsewhere [1, 2; 4–6].

Theoretical studies of the problem of radial end-constraint have not been completely successful because of the mathematical complexity of the problem. FILON [9] presented the first approximate solution to the radially end-constrained cylinder where no radial displacement along the perimeter of the specimen ends was permitted. While his solution gives results in general agreement with experimental results [5], exact numerical confirmation of the stress magnitudes does not exist. This discrepancy is particularly true near and on the end surface of the specimen. While some of this discrepancy is due to the approximate nature of Filon's solution, it can be shown that his solution does, in fact, diverge at the contact surface ([9], p. 189). BALLA [3] attempted to improve on Filon's solution by permitting a variable radial displacement along the ends of the specimen. However, the same arguments against the Filon solution hold true for Balla's solution ([3], p. 64) with the additional argument that his solution gives a finite value of the shear and radial stresses along the perimeter of the specimen at the contact surface. This condition violates the force equilibrium condition. PICKETT [12] presented an exact theoretical calculation of the stresses and displacements in the specimen. He assumed that the ends do not expand at any point along the contact surface, i.e. radial slipping at the planes of contact with the testing machine does not occur and the end-plates have a ν/E value equal to zero. However, Pickett's solution does not satisfy uniquely the boundary condition that the ends of the specimen do not expand at any point. This leads to a discontinuity in the surface values of the radial and tangential stresses at the ends of the specimen and violates the boundary condition that no radial stress exists along the surface of the specimen ([12], equations (14) and (15)]. Consequently, there is not at present a unique exact theoretical solution to the classical problem of radial end-constraint as originally proposed by Filon.

This paper is part of a continuing study by the Bureau of Mines of the problem of end-effects which arise in laboratory testing of cylindrical specimens of rock. The objective of this paper is to present an exact theoretical solution for the stress and displacement distribution within a radially end-constrained cylindrical specimen compressed axially between rough end-plates and subjected to confining pressure applied to the lateral surface of the specimen.

STATEMENT OF THE PROBLEM

The theoretical problem to be solved is the determination of the stresses and displacements in a circular cylindrical specimen of diameter $2a$ and height $2b$, when the ends of the specimen are deformed axially between rough cylindrical end-plates of different elastic properties than the specimen. The sides of the specimen are subjected to a uniform hydrostatic pressure P_0. The axial force applied to the ends of the specimen is equal to $\pi a^2 \sigma_0$, where σ_0 is the axial stress which would exist in the specimen if there were no end-effects. It is assumed that the specimen is a homogeneous, isotropic, and perfectly elastic solid and

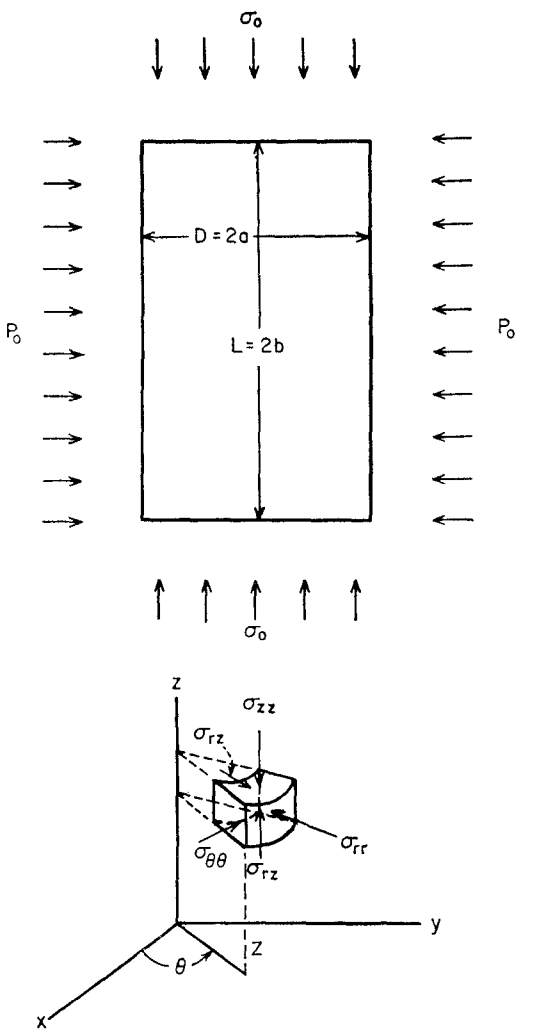

FIG. 1. Specimen geometry, coordinate system, and associated nomenclature.

that the ends of the specimen are parallel to each other and normal to the axis of the specimen. Figure 1 defines the cylindrical coordinates r, θ, and z, gives the nomenclature for the geometry of the specimen and end-plate, and illustrates the general loading conditions.

BOUNDARY CONDITIONS

We shall consider the cylindrical specimen to be subject to the following five boundary conditions:

1. The total force applied to the ends of the specimen is $\pi a^2 \sigma_0$.
2. The radial and axial displacements, u and w, in the specimen must satisfy the symmetry conditions [9]:

u: odd in r; even in z
w: even in r; odd in z.

3. The ends of the specimen are constrained to remain plane, i.e.

$$w = w_0 b \text{ at } z = \pm b \tag{1}$$

where w_0 is a constant.

4. Across the curved surface ($r = a$) for *all* values of z the radial and shear stresses (σ_{rr} and σ_{rz}) are equal to P_0 and zero, respectively. The hydrostatic pressure applied to the sides of the specimen is P_0 (Fig. 1).

5. The ends of the specimen ($z = \pm b$) undergo a radial deformation specified by the functional relationship $g(r)$ $[0 \leqslant r \leqslant a]$. If $J_1(\beta_n r)$ $(n = 1,2. . .)$ represents a Bessel function of the first kind of order one and the β_n are constants whose values are determined by solving the equation $J_1(\beta_n a) = 0$, this boundary condition can be written [11]

$$u = g(r) = \sum_{n=1}^{\infty} F_n J_1(\beta_n r), \quad [0 \leqslant r \leqslant a, z = \pm b] \tag{2}$$

where

$$F_n = \frac{2}{a^2} \int_0^a \frac{r g(r) J_1(\beta_n r)\, \mathrm{d}r}{[J'_1(\beta_n a)]^2}$$

$$J'_1(\beta_n a) \equiv \frac{\mathrm{d}}{\mathrm{d}(\beta_n a)} [J_1(\beta_n a)]. \tag{3}$$

METHOD OF SOLUTION

As the radial, tangential, and axial displacements (u, v, w) are independent of the angular coordinate θ (Fig. 1) because of axial symmetry, the displacement differential equations to be solved in the absence of external body forces are [12]

$$\mu \left[\nabla^2 u - \frac{u}{r^2}\right] + (\lambda + \mu) \frac{\partial}{\partial r} \left[\frac{\partial u}{\partial r} + \frac{u}{r} + \frac{\partial w}{\partial z}\right] = 0$$

$$\frac{\partial}{\partial r} \left[\frac{1}{r} \frac{\partial}{\partial r} (rv)\right] + \frac{\partial^2 v}{\partial z^2} = 0 \tag{4}$$

$$\mu \nabla^2 w + (\lambda + \mu) \frac{\partial}{\partial z} \left[\frac{\partial u}{\partial r} + \frac{u}{r} + \frac{\partial w}{\partial z}\right] = 0$$

where μ and λ are the Lamé elastic constants† and ∇^2 is the Laplacian operator defined in cylindrical coordinates to be

$$\nabla^2 \equiv \frac{\partial^2}{\partial r^2} + \frac{1}{r} \frac{\partial}{\partial r}.$$

† If E and ν denote the Young's modulus and Poisson's ratio of an elastic material, the relationships between these quantities and the Lamé constants can be written $\lambda = E\nu/(1+\nu)(1-2\nu)$ and $\mu = E/2(1+\nu)$.

The axial (σ_{zz}), radial (σ_{rr}), tangential ($\sigma_{\theta\theta}$), and shear (σ_{rz}) stresses are related to the displacements u and w by the following equations:

$$\begin{aligned}
\sigma_{zz} &= \lambda\left[\frac{\partial u}{\partial r} + \frac{u}{r}\right] + (\lambda + 2\mu)\frac{\partial w}{\partial z} \\
\sigma_{rr} &= (\lambda + 2\mu)\frac{\partial \mu}{\partial r} + \lambda\left[\frac{\partial w}{\partial z} + \frac{u}{r}\right] \\
\sigma_{\theta\theta} &= (\lambda + 2\mu)\frac{u}{r} + \lambda\left[\frac{\partial w}{\partial z} + \frac{\partial u}{\partial r}\right] \\
\sigma_{rz} &= \mu\left[\frac{\partial w}{\partial r} + \frac{\partial u}{\partial z}\right].
\end{aligned} \tag{5}$$

ANALYSIS

Elementary forms of the particular solutions for the displacements in the cylindrical coordinates r and z in elastic materials are as follows [12]:

$$\begin{aligned}
u &= u_1 + u_2 + u_3 + u_4 \\
w &= w_1 + w_2 + w_3 + w_4
\end{aligned} \tag{6}$$

where

$$\begin{aligned}
u_1 &= \frac{1}{B_n} J_1(\beta_n r)\begin{Bmatrix}\sinh \beta_n z \\ \cosh \beta_n z\end{Bmatrix}; \qquad w_1 = -\frac{1}{\beta_n} J_0(\beta_n r)\begin{Bmatrix}\cosh \beta_n z \\ \sinh \beta_n z\end{Bmatrix} \\
u_2 &= z J_1(\beta_n r)\begin{Bmatrix}\sinh \beta_n z \\ \cosh \beta_n z\end{Bmatrix}; \qquad w_2 = -\frac{1}{\beta_n} J_0(\beta_n r)\begin{Bmatrix}\beta_n z \cosh \beta_n z - \dfrac{\lambda + 3\mu}{\lambda + \mu}\sinh \beta_n z \\ \beta_n \sinh \beta_n z - \dfrac{\lambda + 3\mu}{\lambda + \mu}\cosh \beta_n z\end{Bmatrix} \\
u_3 &= -\frac{1}{\alpha_m} I_1(\alpha_m r)\begin{Bmatrix}\sin \alpha_m z \\ \cos \alpha_m z\end{Bmatrix}; \quad w_3 = \frac{1}{\alpha_m} I_0(\alpha_m r)\begin{Bmatrix}\sin \alpha_m z \\ \cos \alpha_m z\end{Bmatrix} \\
u_4 &= I_0(\alpha_m r)\begin{Bmatrix}\sin \alpha_m z \\ \cos \alpha_m z\end{Bmatrix}; \qquad w_4 = -\frac{1}{\alpha_m}\left[\alpha_m r I_1(\alpha_m r) - 2\frac{\lambda + 2\mu}{\lambda + \mu} I_0(\alpha_m r)\right]\begin{Bmatrix}-\cos \alpha_m z \\ -\sin \alpha_m z\end{Bmatrix}.
\end{aligned} \tag{7}$$

The quantities $J_0(\beta_n r)$ and $J_1(\beta_n r)$ are Bessel functions of the first kind of order zero and

one, respectively, and $I_0(\alpha_m r)$ and $I_1(\alpha_m r)$ are the modified Bessel functions of order zero and one, respectively [11].†

If all the above particular solutions are combined and substituted into equation [4], the general equations for the radial and axial displacements can be written

$$u = u_0 r + \sum_{n=1}^{\infty} J_1(\beta_n r)\left[A_n z \sinh \beta_n z + \frac{B_n}{\beta_n}\cosh \beta_n z\right] + \sum_{m=1}^{\infty} \frac{C_m \cos \alpha_m z}{I_1(\alpha_m a)}\left\{\left[\frac{\lambda + 2\mu}{(\lambda + \mu)\alpha_m a} + \frac{I_0(\alpha_m a)}{I_1(\alpha_m a)}\right] a I_1(\alpha_m r) - r I_0(\alpha_m r)\right\} \tag{8}$$

$$w = w_0 z + \sum_{n=1}^{\infty} \frac{J_0(\beta_n r)}{\beta_n}\left[A_n\left(\frac{\lambda + 3\mu}{\lambda + \mu}\sinh \beta_n z - \beta_n z \cosh \beta_n z\right) - B_n \sinh \beta_n z\right] + \sum_{m=1}^{\infty} \frac{C_m \sin \alpha z}{I_1(\alpha_m a)}\left\{r I_1(\alpha_m r) + \left[\frac{\lambda + 2\mu}{(\lambda + \mu)\alpha_m a} - \frac{I_0(\alpha_m a)}{I_1(\alpha_m a)}\right] a I_0(\alpha_m r)\right\}$$

where A_n, B_n, C_n, β_n and α_m are constants to be evaluated from the boundary conditions.

The constants β_n and α_m in equation (7) can be evaluated from the boundary condition that the shear stress (σ_{zz}) is zero at all points on the curved surface of the specimen. Combining equation (5) for the shear stress and equation (8) for the displacements gives

$$\begin{aligned} \sin \alpha_m b &= 0 \qquad (m = 0, 1, 2, \ldots) \\ J_1(\beta_n a) &= 0 \qquad (n = 0, 1, 2, \ldots) \end{aligned} \tag{9}$$

where $\alpha_m = m\pi/b$ $(m = 0, 1, 2\ldots)$ and the constants β_n denote the zeros of $J_1(\beta_n r)$[11]. The result is

$$u = g(r) = \sum_{n=1}^{\infty} \frac{1}{r} g(r) \bar{B}_n J_1(\beta_n r) \tag{10}$$

where

$$\bar{B}_n = \frac{2}{a^2}\frac{\int_0^a r^2 J_1(\beta_n r)\,\mathrm{d}r}{[J'_1(\beta_n a)]^2} = -\frac{2}{\beta_n J_0(\beta_n a)} \quad (n = 1, 2, \ldots) \tag{11}$$

† The unmodified and modified Bessel functions of the first kind and orders are defined to be

$$J_s(\beta_n r) = \sum_{r=0}^{\infty} (-1)^r \frac{(\beta_n r/2)^{s+2r}}{r!\,\Gamma(s + r + 1)}$$

$$I_s(\alpha_m r) = \sum_{r=0}^{\infty} \frac{(\alpha_m r/2)^{s+2r}}{r!\,\Gamma(s + r + 1)}$$

where $\Gamma(s + r + 1)$ is the gamma function $\left[\Gamma(s + r + 1) \equiv \int_0^{\infty} t^{(s+r)} \mathrm{e}^{-t}\,\mathrm{d}t\right]$.

with

$$J'_1(\beta_n a) \equiv \frac{\mathrm{d}}{\mathrm{d}(\beta_n a)}[J_1(\beta_n a)].$$

Consequently, equation (8) for the radial displacement at $z = \pm b$ can be rearranged to read

$$0 = \sum_{n=1}^{\infty} J_1(\beta_n r)\left[A_n b \sinh\beta_n b + \frac{B_n}{\beta_n}\cosh\beta_n b + (\epsilon^* + u_0)\bar{B}_n\right] + \sum_{m=1}^{\infty}\frac{C_m \cos\alpha_m b}{I_1}\left\{\left[\frac{\lambda+2\mu}{(\lambda+\mu)\alpha_m a} + \frac{I_0}{I_1}\right] aI_1(\alpha_m r) - rI_0(\alpha_m r)\right\} \tag{12}$$

where

$$I_0 \equiv I_0(\alpha_m a),\ I_1 \equiv I_1(\alpha_m a),\ \epsilon^* = \frac{2}{a^2 J_0^2}\int_0^a g(r) J_1^2(\beta_n r)\,\mathrm{d}r \text{ and } J_0 \equiv J_0(\beta_n a).$$

If both sides of equation (12) are multiplied by $rJ_1(\beta_n r)$ and integrated over the interval $(0, a)$, the following relationship between the constants A_n, B_n and C_m is obtained:

$$A_n b \sinh\beta_n b + \frac{B_n}{\beta_n}\cosh\beta_n b = -(\epsilon^* + u_0)\bar{B}_n - \frac{2Z_{mn}}{a^2 J_0^2}, \quad n \geqslant 1 \tag{13}$$

where

$$Z_{mn} = \sum_{m=1}^{\infty} C_m \frac{\cos\alpha b}{I_1}\int_0^a \left\{\left[\frac{\lambda+2\mu}{(\lambda+\mu)\alpha_m a} + \frac{I_0}{I_1}\right] aI_1(\alpha_m r) - rI_0(\alpha_m r)\right\} rJ_1(\beta_n r)\,\mathrm{d}r. \tag{14}$$

Evaluation of the integral in equation (14) gives

$$Z_{mn} = \sum_{m=1}^{\infty} C_m(-1)^{m+1} a^3 \frac{\Delta}{(\alpha_m a)^2(1+\Delta^2)} J_0\left[\frac{\lambda+2\mu}{\lambda+\mu} + \frac{2}{1+\Delta^2}\right] \tag{15}$$

where $\Delta \equiv \beta_n/\alpha_m$.

The relationship between the constants A_n and B_n can be found by applying the boundary condition that the axial displacement is a constant at the ends of the specimen, i.e. $w = w_0 b$ at $z = \pm b$. The result is

$$B_n = A_n\left(\frac{\lambda+3\mu}{\lambda+\mu} - b\beta_n \coth\beta_n b\right), (n \geqslant 1). \tag{16}$$

The constants A_n and B_n can now be written in terms of the constant C_m as

$$A_n = \frac{\left[(\epsilon^* + u_0)\bar{B}_n + \frac{2Z_{mn}}{a^2 J_0^2}\right]\sinh\beta_n b}{b\left[1 - \left(\frac{\lambda+3\mu}{\lambda+\mu}\right)\frac{\sinh 2\beta_n b}{2\beta_n b}\right]}$$

$$B_n = \frac{\left[(\epsilon^* + u_0)\bar{B}_n + \frac{2Z_{mn}}{a^2 J_0^2}\right]\left[\frac{\lambda+3\mu}{\lambda+\mu}\sinh\beta_n b - b\beta_n\cosh\beta_n b\right]}{b\left[1 - \left(\frac{\lambda+3\mu}{\lambda+\mu}\right)\frac{\sinh 2\beta_n b}{2\beta_n b}\right]}. \tag{17}$$

The stress distribution equations can now be found from the stress–displacement relations, namely

$$\sigma_{rr} = \lambda w_0 + 2(\lambda+\mu)\,u_0 + 2\mu \sum_{n=1}^{\infty} A_n J_0(\beta_n r)\left[\beta_n z \sinh \beta_n z + \frac{\lambda}{\lambda+\mu}\cosh \beta_n z + \cosh \beta_n z \left(\frac{\lambda+3\mu}{\lambda+\mu} - b\beta_n \coth \beta_n b\right)\right] - 2\mu \sum_{n=1}^{\infty} A_n \frac{J_1(\beta_n r)}{r}\left[z \sinh \beta_n z + \frac{1}{\beta_n}\cosh \beta_n z \left(\frac{\lambda+3\mu}{\lambda+\mu} - b\beta_n \coth \beta_n b\right)\right] - 2\mu \sum_{n=1}^{\infty} \frac{C_m \cos \alpha_m z}{I_1}\left[\alpha_m r I_1(\alpha_m r) - \left(1 + \frac{\alpha_m a I_0}{I}\right) I_0(\alpha_m r) + \left(\frac{\lambda+2\mu}{\lambda+\mu} + \frac{\alpha_m a I_0}{I_1}\right)\frac{I_1(\alpha_m r)}{\alpha_m r}\right] \tag{18}$$

$$\sigma_{\theta\theta} = \lambda w_0 + 2(\lambda+\mu)\,u_0 + 2\mu \sum_{n=1}^{\infty} A_n J_0(\beta_n r)\frac{\lambda}{\lambda+\mu}\cos \beta_n z + 2\mu \sum_{n=1}^{\infty} A_n \frac{J_1(\beta_n r)}{r}\left[z \sinh \beta_n z + \frac{1}{\beta_n}\cosh \beta_n z \left(\frac{\lambda+3\mu}{\lambda+\mu} - b\beta_n \coth \beta_n b\right)\right] + 2\mu \sum_{m=1}^{\infty} \frac{C_m \cos \alpha_m z}{I_1}\left[\left(\frac{\lambda+2\mu}{\lambda+\mu} + \frac{\alpha_m a I_0}{I_1}\right)\frac{I_1(\alpha_m r)}{\alpha_m r} - \frac{\mu}{\lambda+\mu} I_0(\alpha_m r)\right] \tag{19}$$

$$\sigma_{zz} = (\lambda+2\mu)\,w_0 + 2\lambda\,u_0 + 2\mu \sum_{n=1}^{\infty} A_n J_0(\beta_n r)\left[\left(\frac{\lambda+2\mu}{\lambda+\mu}\cosh \beta_n z - \beta_n z \sinh \beta_n z\right) - \cosh \beta_n z \left(\frac{\lambda+3\mu}{\lambda+\mu} - b\beta_n \coth \beta_n b\right)\right] + 2\mu \sum_{m=1}^{\infty} \frac{C_m \cos \alpha_m z}{I_1}\left[\alpha_m r I_1(\alpha_m r) + \left(2 - \frac{\alpha_m a I_0}{I_1}\right) I_0(\alpha_m r)\right]. \tag{20}$$

$$\sigma_{rz} = 2\mu \sum_{n=1}^{\infty} A_n J_1(\beta_n r)\frac{(\lambda+2\mu)}{\lambda+\mu}\sinh \beta_n z + 2\mu \sum_{m=1}^{\infty} \frac{C_m \sin \alpha_m z}{I_1}\left[\alpha_m r I_0(\alpha_m r) - \frac{\alpha_m a I_0}{I_1} I_1(\alpha_m r)\right]. \tag{21}$$

Notice that the shear stress (σ_{rz}) is identically zero whenever $r = \pm a$. When $z = \pm b$, σ_{rr} is zero for $r = 0$ and $r = a$. Therefore, all boundary conditions of σ_{rz} are met exactly.

If we apply the boundary condition that $\sigma_{rr} = P_0$ for all values of z along the specimen surface, then

$$P_0 = \lambda w_0 + 2(\lambda + \mu)\, u_0 + 2\mu \sum_{n=1}^{\infty} A_n J_0 \left[\beta_n z \sinh \beta_n z + \frac{\lambda}{\lambda + \mu} \cosh \beta_n z + \left(\frac{\lambda + 3\mu}{\lambda + \mu} - b\beta_n \coth \beta_n b\right) \cosh \beta_n z\right] - 2\mu \sum_{m=1}^{\infty} \frac{C_m \cos \alpha_m z}{I_1} \left[\alpha_m a I_1 - \left(1 + \frac{\alpha_m a I_0}{I_1}\right) I_0 + \left(\frac{\lambda + 2\mu}{\lambda + \mu} + \frac{\alpha_m a I_0}{I_1}\right) \frac{I_1}{\alpha_m a}\right]. \tag{22}$$

We can now expand the terms $\beta_n z \sinh \beta_n z$ and $\cosh \beta_n z$ in terms of $\cos \alpha_m z$ i.e.

$$\begin{aligned} \beta_n z \sinh \beta_n z &= a_{0n} + \sum_{m=1}^{\infty} a_{mn} \cos \alpha_m z \\ \cosh \beta_n z &= b_{0n} + \sum_{m=1}^{\infty} b_{m1} \cos \alpha_m z \end{aligned} \tag{23}$$

where

$$\begin{aligned} a_{0n} &= \frac{1}{\beta_n b} [\beta_n b \cosh \beta_n b - \sinh \beta_n b] \\ b_{0n} &= \frac{1}{\beta_n b} \sinh \beta_n b \\ a_{mn} &= -\frac{2}{\beta_n b} \frac{[1 - (\alpha_m/\beta_n)^2]}{[1 + (\alpha_m/\beta_n)^2]} \sinh \beta_n b \cos \alpha_m b \\ b_{mn} &= \frac{2}{\beta_n b} \frac{\sinh \beta_n n \cos \alpha_m b}{1 + (\alpha_m/\beta_n)^2}. \end{aligned} \tag{24}$$

If we insert equation (24) into equation (22) and equate like terms, two additional relationships between the unknown constants result:

$$\lambda w_0 + 2(\lambda + \mu)\, u_0 = P_0 - 2\mu \sum_{n=1}^{\infty} A_n J_0 \left[\left(a_{0n} + b_{0n} \frac{\lambda}{\lambda + \mu}\right) + b_{0n} \left(\frac{\lambda + 3\mu}{\lambda + \mu} - b\beta_n \coth \beta_n b\right)\right] \tag{25}$$

$$C_m = \frac{\sum_{n=1}^{\infty} A_n J_0 \left[\left(a_{mn} + \frac{\lambda}{\lambda + \mu} b_{mn}\right) + b_{mn} \left(\frac{\lambda + 3\mu}{\lambda + \mu} - b\beta_n \coth \beta_n b\right)\right]}{\frac{1}{I_1} \left[\alpha_m a I_1 - \left(1 + \frac{\alpha_m a I_0}{I_1}\right) I_0 + \left(\frac{\lambda + 2\mu}{\lambda + \mu} + \frac{\alpha_m a I_0}{I_1}\right) \frac{I_1}{\alpha_m a}\right]}.$$

There are now six relationships—equations (9), (16), (20), (25)—between the seven unknown constants (α_m, β_n, A_n, B_n, C_m, u_0, w_0). The remaining equation is found by applying the

force equilibrium condition in the axial direction, i.e. if σ_0 is the value of the applied axial stress when there is no end-effect

$$2\pi \int_0^a r\sigma_{zz}\, dr = \pi a^2 \sigma_0 \quad z = \pm b \tag{26}$$

where σ_{zz} is given by equation (20) with z replaced by $\pm b$. If equation (20) with z replaced by $\pm b$ is substituted into equation (26) and the indicated integration is performed, the relationship between the constants u_0 and w_0 is

$$2\lambda u_0 + (\lambda + 2\mu) w_0 = \sigma_0. \tag{27}$$

Therefore the constants in the series expansions for the displacements and stresses in the specimen can be written

$$A_n = \frac{\left[(\epsilon^* + u_0)\, \bar{B}_n + \dfrac{2Z_{mn}}{a^2 J_0^2}\right] \sinh \beta_n b}{b\left[1 - \left(\dfrac{\lambda + 3\mu}{\lambda + \mu}\right) \dfrac{\sinh 2\beta_n b}{2\beta_n b}\right]} \tag{28a}$$

$$B_n = A_n \left[\frac{\lambda + 3\mu}{\lambda + \mu} - b\beta_n \coth \beta_n b\right] \tag{28b}$$

$$C_m = \frac{\sum_{n=1}^{\infty} A_n h_n(b) J_0}{F(\alpha_m a)} \tag{28c}$$

$$u_0 = \frac{P_0 - \dfrac{\lambda\sigma_0}{\lambda + 2\mu} + 2\mu \sum_{n=1} J_0 \dfrac{f_n(b)}{g_n(b)} \left[\epsilon^* \bar{B}_n + \dfrac{2Z_{mn}}{a^2 J_0^2}\right]}{2(\lambda + \mu) - \dfrac{2\lambda^2}{\lambda + \sigma\mu} - 2\mu \sum_{n=1}^{\infty} J_0 \dfrac{f_n(b)}{g_n(b)} \bar{B}_n} \tag{28d}$$

$$w_0 = \frac{\sigma_0 - 2\lambda u_0}{\lambda + 2\mu} \tag{28e}$$

where

$$\epsilon^* = \frac{2}{a^2 J_0^2} \int_0^a g(r) J_1^2(\beta_n r)\, dr$$

$$f_n(b) = a_{0n} + b_{0n}\left(\frac{2\lambda + 3\mu}{\lambda + \mu} - b\beta_n \coth \beta_n b\right)$$

$$g_n(b) = b \sinh \beta_n b + \frac{1}{\beta_n} \cosh \beta_n b \left(\frac{\lambda + 3\mu}{\lambda + \mu} - b\beta_n \coth \beta_n b\right) \tag{29}$$

$$h_n(b) = a_{mn} + b_{mn}\left(\frac{2\lambda + 3\mu}{\lambda + \mu} - b\beta_n \coth \beta_n b\right)$$

$$F(\alpha_m a) = \frac{1}{I_1}\left[\alpha_m a I_1 - \left(1 + \frac{\alpha_m a I_0}{I_1}\right) I_0 + \left(\frac{\lambda + 2\mu}{\lambda + \mu} + \frac{\alpha_m a I_0}{I_1}\right) \frac{I_0}{\alpha_m a}\right].$$

The constants a_{0n}, a_{m0}, b_{0n}, b_{mn}, α_m, and β_n have been defined earlier [see equations (9) and (24)].

To qualitatively check the above equations we consider first the stresses at the geometrical center of the specimen $(z/b) = (r/a) = 0$. Let the L/D or b/a value of the specimen increase to large values. We see from equation (28) that the constants A_n, B_n and C_m all approach zero and

$$\lambda w_0 + 2(\lambda + \mu) u_0 = P_0$$

and

$$2\lambda u_0 + (\lambda + 2\mu) w_0 = \sigma_0.$$

Consequently the stresses $(\sigma_{zz}, \sigma_{rr}, \sigma_{\theta\theta}, \sigma_{rz})$ approach the equilibrium values (i.e. no radial end-effect) of $(\sigma_0, P_0, P_0, 0)$. Next let the L/D or b/a value of the specimen approach zero. The constant w_0 approaches $\sigma_0/(\lambda+2\mu)$. The stresses $(\sigma_{zz}, \sigma_{rr}, \sigma_{\theta\theta}, \sigma_{rz})$ become $(\sigma_0, \sigma_0\nu/(1-\nu), \sigma_0\nu/1-\nu), 0$, where ν is the Poisson's ratio. These stress values for these extreme limiting cases agree with the values obtained by the finite element method of solution[5].

NUMERICAL EVALUATIONS

The stresses and displacements in the specimen are found by calculating the constants in equation (28). The values of the constants A_n, B_n, C_m, u_0 and w_0 are determined by substituting equation (28d) into (28a). Equations (28a) and (28c) are solved simultaneously for the C_m. The known values of the C_m are then substituted into equations (28a)–(28e) to determine the A_n, B_n, u_0 and w_0. The radial displacement distribution $[g(r)]$ along the ends of the specimen must be specified in order to perform these calculations.

To check the theoretical solution, four terms of the A_n, B_n and C_m series were evaluated. The L/D value of the specimen was 2·00. The Young's modulus and Poisson's ratio (ν) of the specimen were 2×10^6 psi and 0·24, respectively. The radial displacement function, $g(r)$, was taken to be $2{\cdot}04 \times 10^{-8} r\sigma_0$. It has been shown [6] that this displacement function corresponds to the case of a cylindrical specimen with elastic moduli E and ν to 30×10^6 psi and 0·24, respectively, compressed axially between rough end-plates (of the same diameter as the specimen) with elastic moduli E and ν equal to 30×10^6 psi and 0·30, respectively. Figure 2 shows the results of the theoretical calculations (dashed lines). The results of the solution of this problem solved by the finite-element method of solution are shown for comparison (solid lines). The conclusion to be obtained from this figure is that the agreement between the finite element and theoretical solutions is good even though only four terms of the series were evaluated for the theoretical solution.

THE SURFACE DISPLACEMENT FUNCTION $g(r)$

An exact theoretical solution of the stress and displacement distribution in a radially end-constrained circular cylinder requires a knowledge of the radial displacement function $[g(r)]$ along the end surfaces $(z = \pm b)$ of the cylinder. This function can be calculated exactly by using equation (7) to solve the general problem of a cylindrical specimen loaded axially between rough end-plates, provided both the geometry and the elastic properties of the specimen and end-plates are specified. This problem is difficult to solve and for all practical purposes this approach is mathematically intractable. Another and more practical approach is to estimate the functional form of $g(r)$. There are two methods of estimating this function, namely the experimental and empirical methods. In the experimental method a

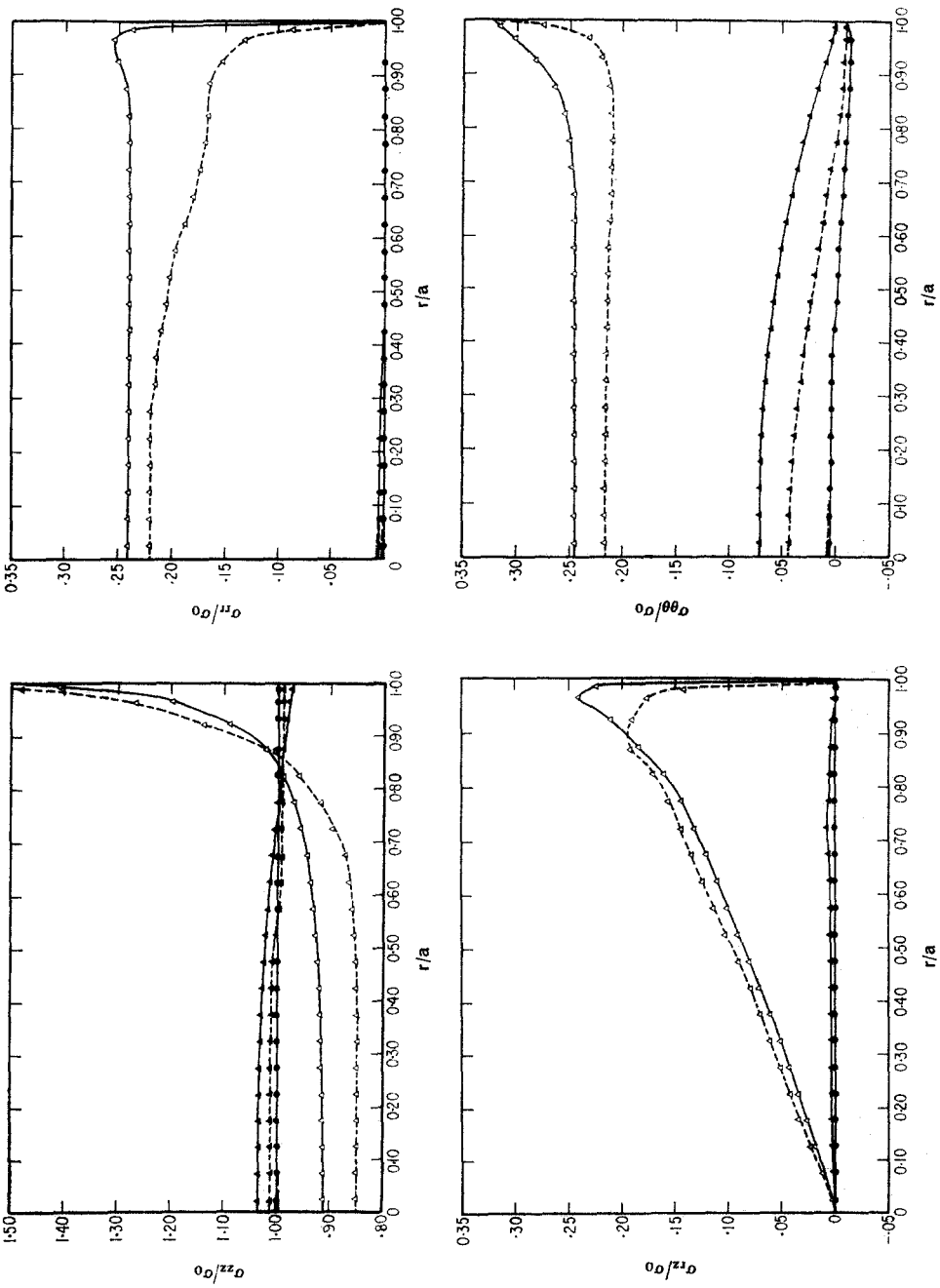

FIG. 2. Comparison of the theoretical (dashed line) and finite element (solid line) solutions for the stress distribution in the radially end-constrained cylinder [$g(r) = 2{\cdot}04 \times 10^{-8}\, r\sigma_0$].
● $z/b = 0{\cdot}00$; ▲ $z/b = 0{\cdot}50$; △ $z/b = 1{\cdot}00$

knowledge is required of the displacements on the surface ($r = a$) of the cylinder. For example, a value of $g(r)$ is substituted into equations (8), (28) and (29), and the calculated displacements are compared with the measured displacements. If the calculated values are different from the measured values, a new value of $g(r)$ is used and the displacements are recalculated. This procedure is continued until the calculated displacements converge to the measured displacements. This method requires the function $g(r)$ to vary linearly with the radial distance r ($0 \leqslant r \leqslant a$). Application of the finite element method of solution to this problem [4,5] has shown that $g(r)$ does vary linearly (for a wide range of Young's modulus for the specimen) across the ends of the specimen, provided there is no relative movement between the specimen and end-plate. In the empirical method an estimate is made of the functional form of $g(r)$. A lower bound on $g(r)$ is easily obtained by equating the radial strain along the ends ($z = \pm b$) of the specimen to the radial strain that would exist in the end-plate if it were free to expand in the radial direction. Similarly an upper bound on $g(r)$ is obtained by equating the radial strain along the specimen ends to the radial strain that would exist in the specimen if it were free to expand in the radial direction. Therefore, the function (gr) must satisfy the inequality

$$\epsilon_{rr}^{(p)} \leqslant \frac{1}{r} g(r) \leqslant \epsilon_{rr}^{(s)} \quad (0 \leqslant r \leqslant a, z = \pm b) \tag{30}$$

where the quantities $\epsilon_{rr}^{(p)}$ and $\epsilon_{rr}^{(s)}$ refer to the unconstrained values of the radial strains in the end-plate and specimen, respectively. In the case of uniaxial loading equation (30) becomes

$$\frac{\nu_p}{E_p} \sigma_0 r \leqslant g(r) \leqslant \frac{\nu_s}{E_s} \sigma_0 r \tag{31}$$

where E_p and ν_p and E_s and ν_s are the Young's modulus and Poisson's ratio of the end-plate and specimen, respectively.

The values of the Young's moduli and Poisson's ratios for the end-plate and specimen were taken to be $E_p = 30 \times 10^6$ psi, $\nu = 0{\cdot}30$, $E_s = 2 \times 10^6$ psi, and $\nu_s = 0{\cdot}24$ in the example illustrated in Fig. 2. The substitution of these values into equation (31) gives the bounds on $g(r)$ to be

$$1 \times 10^{-8} \sigma_0 r \leqslant g(r) \leqslant 12 \times 10^{-8} \sigma_0 r.$$

The value of $g(r)$ determined independently by the finite-element method of solution is $2{\cdot}04 \times 10^{-8} \sigma_0 r$ [6].

BRADY and BLAKE [5] found a closer apparent lower bound on the function $g(r)$ by calculating the harmonic mean of $\epsilon_{rr}^{(s)}$ and $\epsilon_{rr}^{(p)}$, i.e.

$$\frac{2}{\frac{1}{r} g^*(r)} = \frac{1}{\epsilon_{rr}^{(s)}} + \frac{1}{\epsilon_{rr}^{(p)}} \tag{32}$$

where the superscript * is the value of the harmonic mean. If the above values of Young's moduli and Poisson's ratios for the end-plate and specimen are substituted into equation (32), the harmonic mean of $g(r)$ is $1{\cdot}85 \times 10^{-8} \sigma_0 r$ for uniaxial loading. We have used a value of $g(r)$ equal to $1{\cdot}85 \times 10^{-8} \sigma_0 r$ in the theoretical analysis and have found an increase in the stresses (σ_{rr}, $\sigma_{\theta\theta}$, σ_{zz}, σ_{rz}) amounting to less than 1 per cent of the theoretically determined stress values shown in Fig. 2. These results show that (for the range of E_s values investigated) equation (32) forms a close approximation of the radial displacement function [$g(r)$] along the ends of the specimen.

CONCLUSIONS

An exact theoretical solution has been presented for determining the stresses and displacements in an elastic cylindrical specimen with prescribed radial displacements along the ends of the specimen. The solution was used to solve the problem of the deformation of a specimen compressed axially between rough end-plates (no slippage between the contact surfaces) of the same diameter as the specimen. It was shown that the stresses in the specimen predicted by the theoretical solution are in agreement with the values given by a finite element study of this problem.

REFERENCES

1. NEWMAN K. and LACHANCE L. The testing of brittle materials under uniform uniaxial compressive stress. *Proc. Am. Soc. Test. Mater.* **64**, 1044–1067 (1964).
2. SELDENRATH R. and GRAMBERG J. Stress–Strain Relations and Breakage of Rocks, in *Mechanical Properties of Nonmetallic Brittle Materials*, pp. 79–102, Butterworths, London (1958).
3. BALLA A. Stress conditions in triaxial compression. *J. Soil Mech. Fdns Div. Am. Soc. civ. Engrs* 57–84 (1960).
4. BRADY B. T. Effects of inserts on the elastic behavior of cylindrical materials loaded between rough end-plates. *Int. J. Rock Mech. Min. Sci.* To be published.
5. BRADY B. T. and BLAKE W. An Elastic Solution for the Laterally Constrained Circular Cylinder Under Uniaxial Loading, *Proceedings of the Tenth Rock Mechanics Symposium*, Austin, Texas (1970).
6. BRADY B. T. This issue, p. 153.
7. DOUGALL J. An analytical theory of the equilibrium of an isotropic elastic rod of circular section. *Trans. R. Soc. Edinb.* **49**, 895–978 (1913).
8. DURELLI A. J. Distribution of Stresses in Partial Compression, *Proceedings of the Thirteenth Semi-annual Eastern Photoelasticity Conference*, Cambridge, Mass., pp. 25–26 (1941).
9. FILON L. N. G. On the elastic equilibrium of circular cylinders under certain practical systems of load. *Phil. Trans. R. Soc.* Ser. A, **198**, 147–233 (1902).
10. GONNERMAN H. F. Effect of end conditions of cylinder in compression tests of concrete. *Proc. Am. Soc. Test. Mater.* **24**, (II) 1036–1063 (1924).
11. IRVING I. and MULLINEAUX N. *Mathematics in Physics and Engineering*, Academic Press, New York (1959).
12. PICKETT G. Application of the Fourier method to the solution of certain boundary problems in the theory of elasticity. *J. appl. Mech.* **2**, (A) 176–179 (1944).